Status AFN and SpH models

W. Dekeyser, W. Van Uytven, N. Horsten, S. Carli, G. Samaey, M. Baelmans

A hierarchy of neutral models

Advanced fluid neutral models (AFN)

- Efficient (direct) coupling to plasma equations, no MC noise
- Basis for hybrid methods
- Good accuracy in highly collisional regimes

Hybrid fluid-kinetic models

Spatially (SpH)

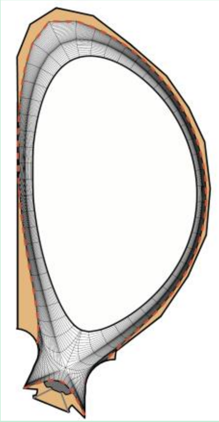

- F-K transition based on location
- User-defined transition criteria

micro-Macro (mMH)

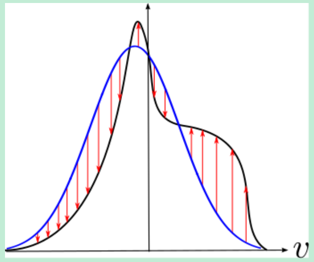

$$f_\mathrm{n}(v) = f_{\mathrm{n,f}}(v) + f_{\mathrm{n,k}}(v)$$

- Decomposition in velocity space
- Can be made fully equivalent to kinetic model

Kinetic model

- Most complete physical description
- Flexibility w.r.t. geometry, collisional processes, sources, boundary conditions,…
- Very expensive in highly collisional regimes

Model accuracy →

← Computational efficiency

CPU × 1/10?

KU LEUVEN

Underlying kinetic equation of current AFN models

$$\frac{\partial f_a(\boldsymbol{r},\boldsymbol{v})}{\partial t} + \boldsymbol{v}\cdot\nabla f_a(\boldsymbol{r},\boldsymbol{v}) + \Sigma_t|\boldsymbol{v}|f_a(\boldsymbol{r},\boldsymbol{v}) = Q_\mathrm{a}(\boldsymbol{r},\boldsymbol{v}) + \int \sigma_{cx}(E_c)|\boldsymbol{v}-\boldsymbol{v}'|f_i(\boldsymbol{r},\boldsymbol{v})f_a(\boldsymbol{r},\boldsymbol{v}')\mathrm{d}\boldsymbol{v}'$$

H, D or T atoms

Atom-plasma reactions

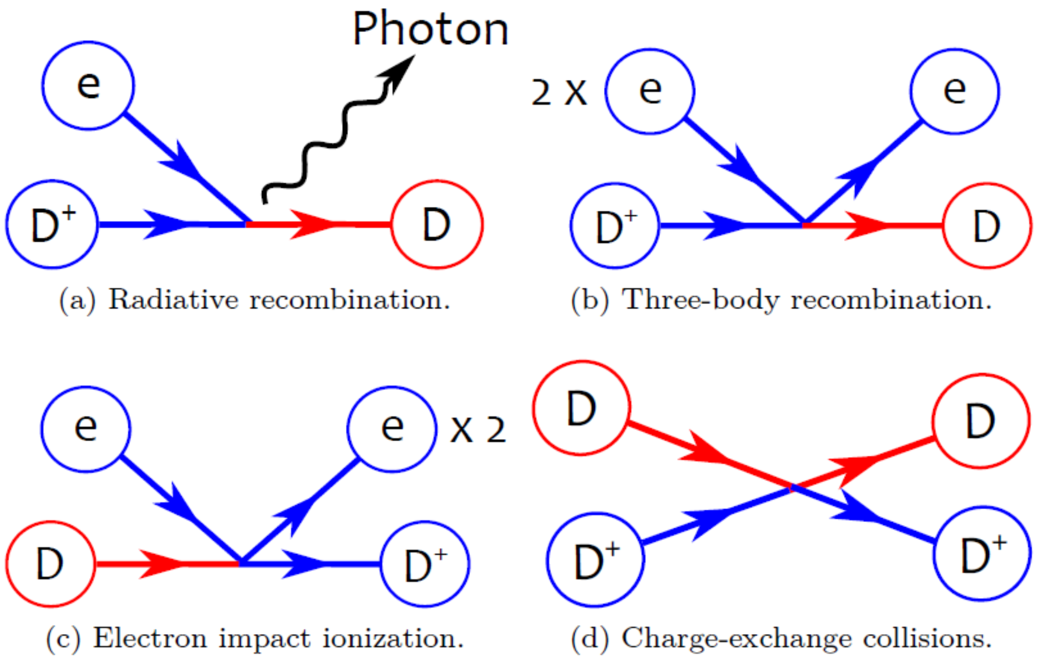

(a) Radiative recombination.
(b) Three-body recombination.
(c) Electron impact ionization.
(d) Charge-exchange collisions.

[Horsten, N., PhD Thesis, 2019]

Boundary conditions

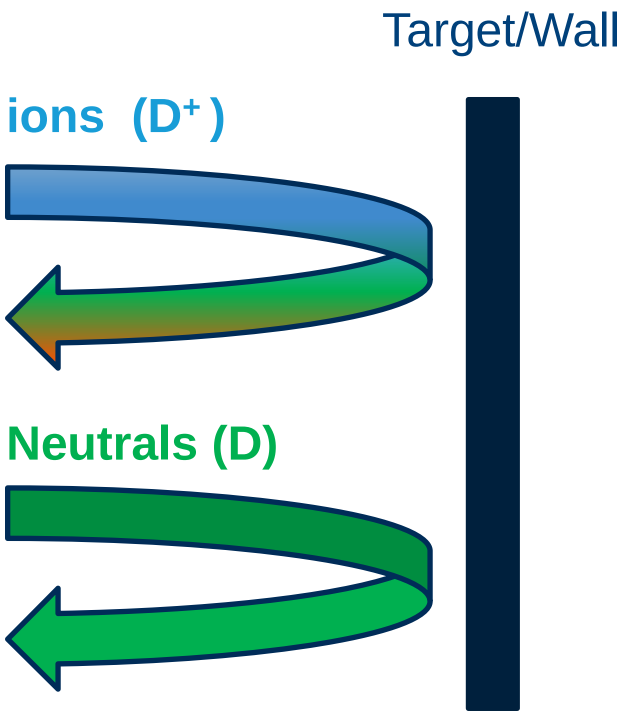

ion recycling
ions: truncated Maxwellian
sheath acceleration

neutral reflection

molecules
Thermal release
or
Immediate dissocation

TRIM database for wall reflection:
$R_F(E',\vartheta',\varphi' \rightarrow E,\vartheta,\varphi)$

KU LEUVEN

Atomic and molecular reactions

Atom-only models (first four reactions)

At target ($D_2 + e \rightarrow 2D + e$)

With molecules (all reactions)

Reaction	Type	AMJUEL
$D^+ + e \rightarrow D + \text{photon}$	Radiative recombination	2.1.8
$D^+ + 2e \rightarrow D + e$	Three-body recombination	2.1.8
$D + e \rightarrow D^+ + 2e$	Ionization	2.1.5
$D + D^+ \rightarrow D^+ + D$	Charge exchange	3.1.8
$D_2 + e \rightarrow D_2^+ + 2e$	Ionization	2.2.9
$D_2 + e \rightarrow 2D + e$	Dissociation	2.2.5g
$D_2 + e \rightarrow D + D^+ + 2e$	Dissociation	2.2.10
$D_2 + D^+ \rightarrow D_2 + D^+$	Elastic scattering	0.3T
$D_2 + D^+ \rightarrow D_2^+ + D$	Ion conversion	3.2.3
$D_2^+ + e \rightarrow D + D^+ + e$	Dissociation	2.2.12
$D_2^+ + e \rightarrow 2D^+ + 2e$	Dissociative ionization	2.2.11
$D_2^+ + e \rightarrow 2D$	Dissociative recombination	2.2.14

= default EIRENE reactions except neutral-neutral collisions

Resulting fluid model

- Following Chapman-Enskog procedure
  [details: see N. Horsten, PhD; and extensions in W. Van Uytven, PhD.]
- Continuity, parallel momentum, and energy equations:

$$\frac{\partial n_\mathrm{a}}{\partial t} + \nabla \cdot \boldsymbol{\Gamma}_\mathrm{a}^n = S_\mathrm{a}^n$$

$$m\,\frac{\partial n_\mathrm{a} V_{\mathrm{a},||}}{\partial t} + \nabla \cdot \boldsymbol{\Gamma}_\mathrm{a}^{||m} + \nabla_{||} p_\mathrm{a} = S_\mathrm{a}^{||m} + S_{CF}^{||m}$$

$$\eta_\mathrm{a} = \frac{p_\mathrm{a}}{(n_\mathrm{i} \boldsymbol{K}_{\mathbf{CX},\boldsymbol{m}} + n_\mathrm{e} K_\mathrm{i})}$$

$$\frac{\partial}{\partial t}\left(\frac{3}{2} n_\mathrm{a} T_\mathrm{a} + \frac{m}{2} n_\mathrm{a} V_{\mathrm{a},||}^2\right) + \nabla \cdot \left(\left(\frac{5}{2} T_\mathrm{a} + \frac{m}{2} n_\mathrm{a} V_{\mathrm{a},||}^2\right)\boldsymbol{\Gamma}_\mathrm{a}^n + \Pi_\mathrm{a} \cdot \boldsymbol{V}_\mathrm{a} + \boldsymbol{q}_\mathrm{a}\right) = S_\mathrm{a}^E$$

$$\kappa_\mathrm{a} = \frac{5\,p_\mathrm{a}}{2\,m\,(n_\mathrm{i} \boldsymbol{K}_{\mathbf{CX},\boldsymbol{m}} + n_\mathrm{e}\,K_\mathrm{i})}$$

- Pressure-diffusion relation for perpendicular directions (perp. mom. eq. simplified to balance pressure gradient vs. momentum sources):

$$\Gamma_{\mathrm{a},\perp}^n = -D_\mathrm{a}^p\,\nabla_\perp p_\mathrm{a} + n_{\mathrm{a},eq}\,V_{\mathrm{i},\perp}$$

Pressure-diffusion coefficient

$$D_\mathrm{a}^p = \frac{1}{m\,(n_\mathrm{i} K_{\mathrm{CX},m} + n_\mathrm{e} K_\mathrm{i})}$$

Equilibrium atom density

$$n_{\mathrm{a},eq} = \frac{(n_\mathrm{i} n_\mathrm{e} K_\mathrm{i} + n_\mathrm{a} n_\mathrm{i} K_{\mathrm{CX},m})}{(n_\mathrm{i} K_{\mathrm{CX},m} + n_\mathrm{e} K_\mathrm{i})}$$

AFN boundary conditions

Speed- and angular-dependent particle flux density

$\Gamma^{\mathrm{n}}_{\nu-}(v,\vartheta,\varphi)$ Incident neutrals: diffusion approx. or Maxwellian approx.

$\Gamma^{\mathrm{i}}_{\nu-}(v,\vartheta,\varphi)$ Incident ions: truncated Maxwellian + sheath acceleration

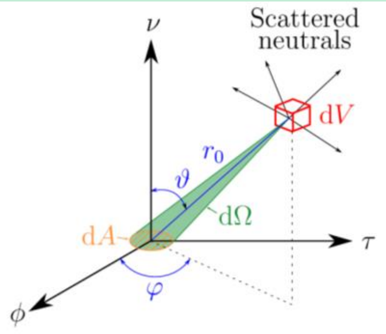

Reflected/recycled neutrals

$$\Gamma^{\mathrm{n}}_{\nu+}(v_{\mathrm{R}},\vartheta_{\mathrm{R}},\varphi_{\mathrm{R}}) = \int_{v=0}^{\infty}\int_{\vartheta=0}^{\pi/2}\int_{\varphi=0}^{2\pi} R(v,\vartheta,\varphi \to v_{\mathrm{R}},\vartheta_{\mathrm{R}},\varphi_{\mathrm{R}}) \sin\vartheta_{\mathrm{R}} (\Gamma^{\mathrm{n}}_{\nu-}(v,\vartheta,\varphi) + \Gamma^{\mathrm{i}}_{\nu-}(v,\vartheta,\varphi))\mathrm{d}v\mathrm{d}\vartheta\mathrm{d}\varphi$$

TRIM database

Moments total distribution: particle, momentum and energy flux densities *[N. Horsten et al., NF* ***57*** *(2017)]*

Diffusion approx.:

- Incident flux: consider neutrals from CX or n-n collisions
- Linearize & integrate over half-space

Maxwellian approx.:

- Indicend flux: assume (drifting) Maxwellian based on T_n and $u_{\|n}$

KU LEUVEN

AFN results – Different wall materials

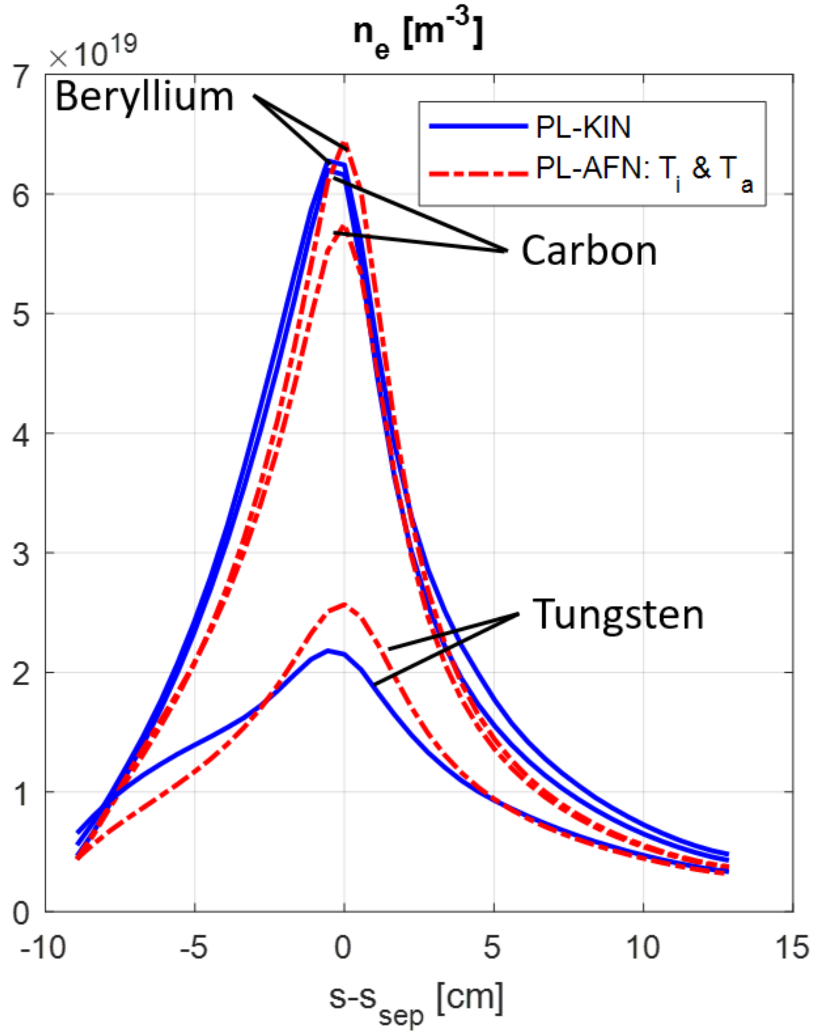

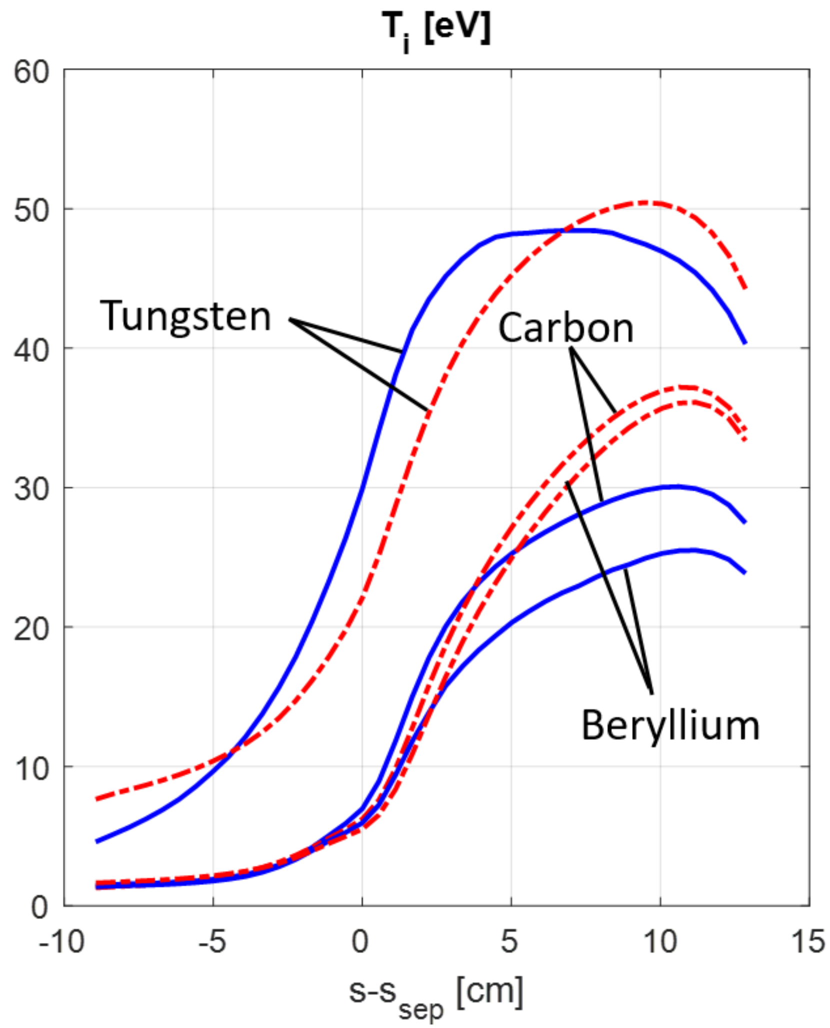

KU LEUVEN

AFN results – ITER W-Be ($n_{i,c} = 8 \cdot 10^{19}\ m^{-3}$)

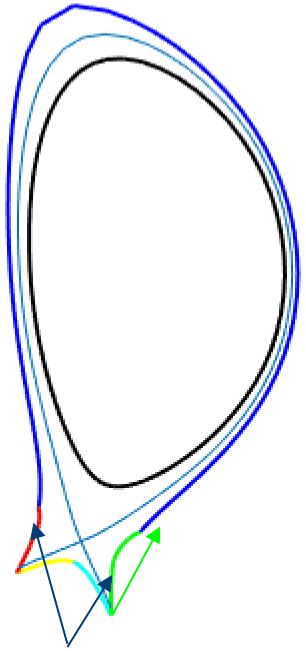

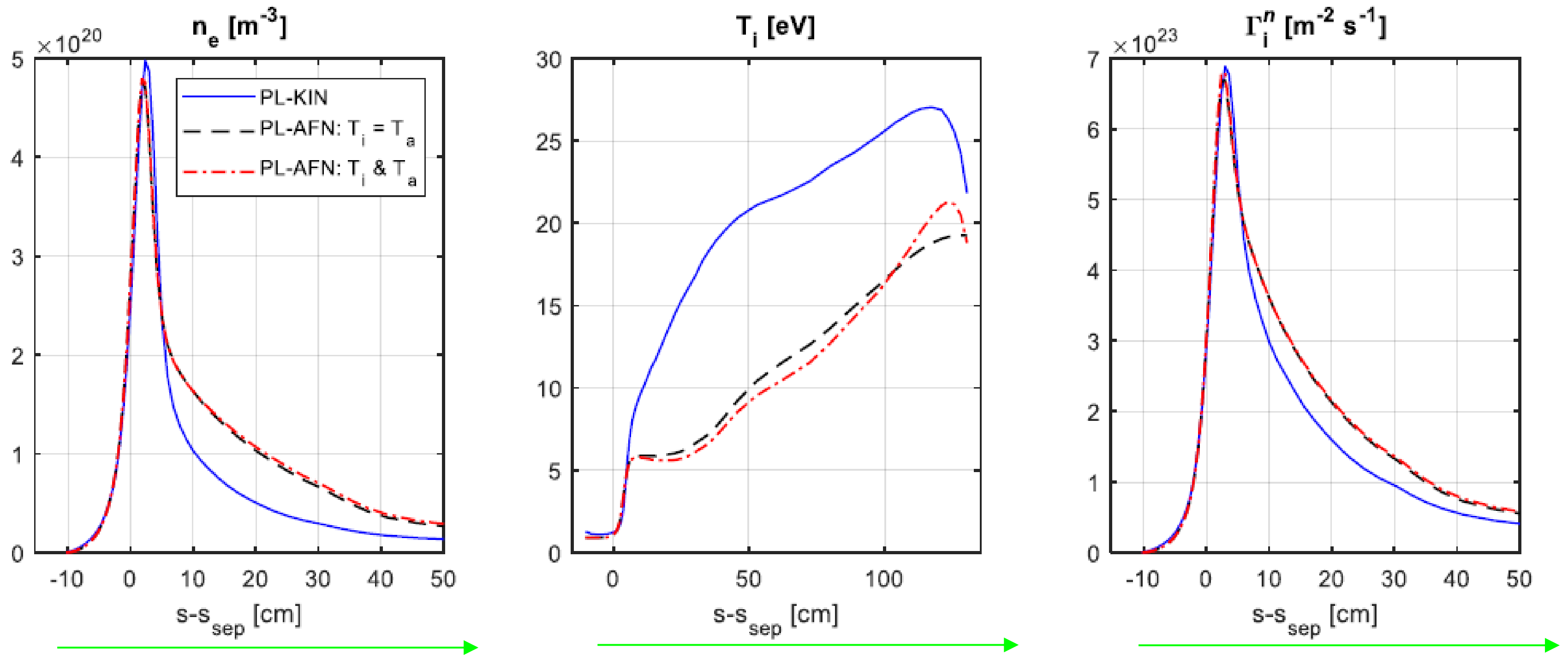

KU LEUVEN

Summary achievements AFN: mature models!

- Significant model improvements compared to ‘standard’ fluid neutral models
  - Transport coefficients consistent with collisional processes used by EIRENE (AMJUEL/HYDHEL) [N. Horsten et al., NF, 2017], including neutral-neutral collision effects [W. Dekeyser et al, PSI, 2024.]
  - Boundary conditions consistent with kinetic EIRENE treatment [N. Horsten et al., NF 57, 2017], incl. fast/thermal reflection (approximate effect of molecules) and TRIM data (effect of wall materials)
  - Separate neutral energy equation to extend validity range of fluid (and SpH) model towards lower recycling conditions [W. Van Uytven et al., CPP 60, 2020]
  - Inclusion of plasma drift effects [W. Van Uytven et al. NME 2022]
- Made widely available to users through implementation in new extended grids version of SOLPS-ITER
  - Correct treatment of grid non-orthogonality [W. Dekeyser et al, NME 18, 2019]
  - Simulations up-to-the-wall [W. Dekeyser et al, NME 27, 2021]
- Already successfully applied to various machines, incl. AUG, JET [N. Horsten et al., NME 2022], ITER [W. Van Uytven et al, NF 62, 2022] and DEMO (link WP-DES) [W. Van Uytven et al, CPP, 2024]
- AFN models implemented in various European turbulence codes (TOKAM3X, GRILLIX – TSVV3).

KU LEUVEN

Three main reasons for fluid-kinetic discrepancies

1. **Fluid grid** does not extend up to the real vessel wall ➔ no neutrals in **void/vacuum regions**

➡ Solved by using extended grid, but low collisionality demands for (partially) kinetic treatment

2. No explicit treatment of **molecules** (H_2) & **impurity species** in AFN model

➡ Not clear if a fluid model is valid

3. Fluid limit is not valid everywhere ➔ **kinetic effects**

➡ Low-collisional regions inside fluid grid

➡ Boundary / first-flight effects

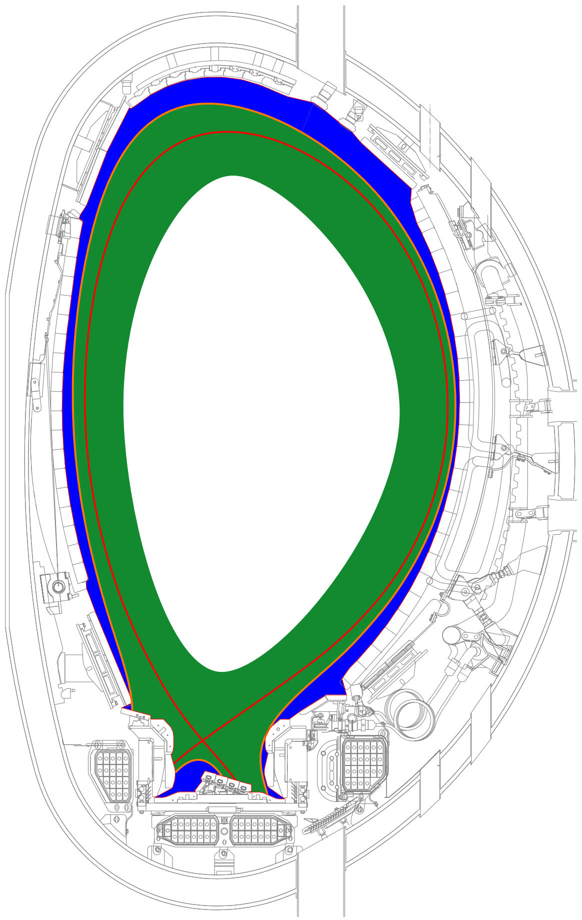

KU LEUVEN

Treatment at plasma-void interfaces

Ion recycling ➔ Also present in fully kinetic simulation

Transition from fluid to kinetic population

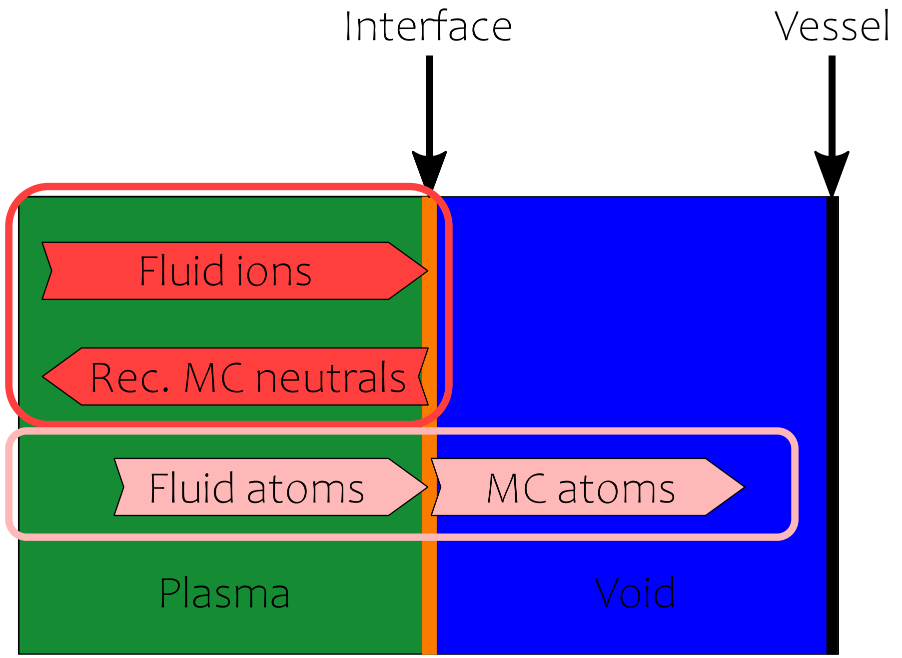

Kinetic atoms are followed until ionization

Important to incorporate some kinetic effects in low-collisional regions (see further)

Fluid neutral boundary condition: Moments of Maxwellian ➔ imposed fluxes:

$$\Gamma_\mu^{\mathrm{n}} = \int_{\mathbf{v}\cdot\boldsymbol{\nu}>0} \mu(\mathbf{v}) M(\mathbf{v}) \mathrm{d}\mathbf{v}$$

Sampled from Maxwellian

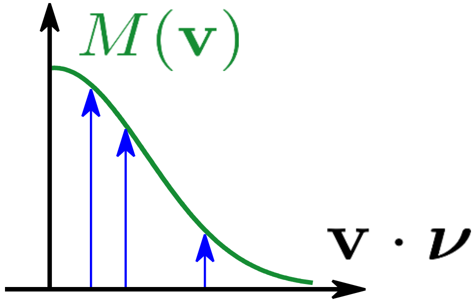

Treatment at wall/divertor boundaries

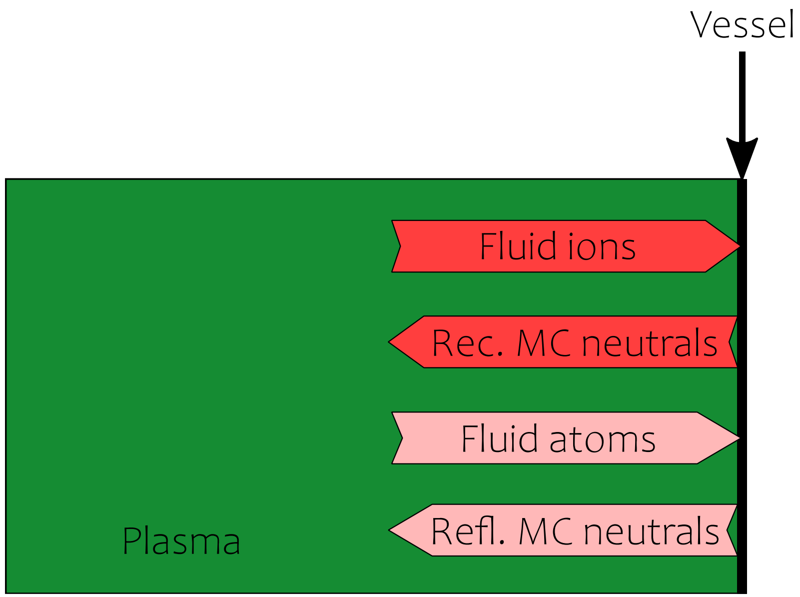

- Launching (all) neutrals kinetically at the vessel walls captures first-flight effects, and significantly improves the agreement with the kinetic reference solution
- Launch as atom (fast recycling) or molecule (thermal desorption)
- Add condensation process to condense kinetic atoms to fluid atoms in highly collisional regions, based on a (user-imposed) transition Knudsen number Kn^t

Maximum hybrid-kinetic discrepancies within 20% for JET L-mode case at the onset of detachment

Outer target profiles:

First-flight effects

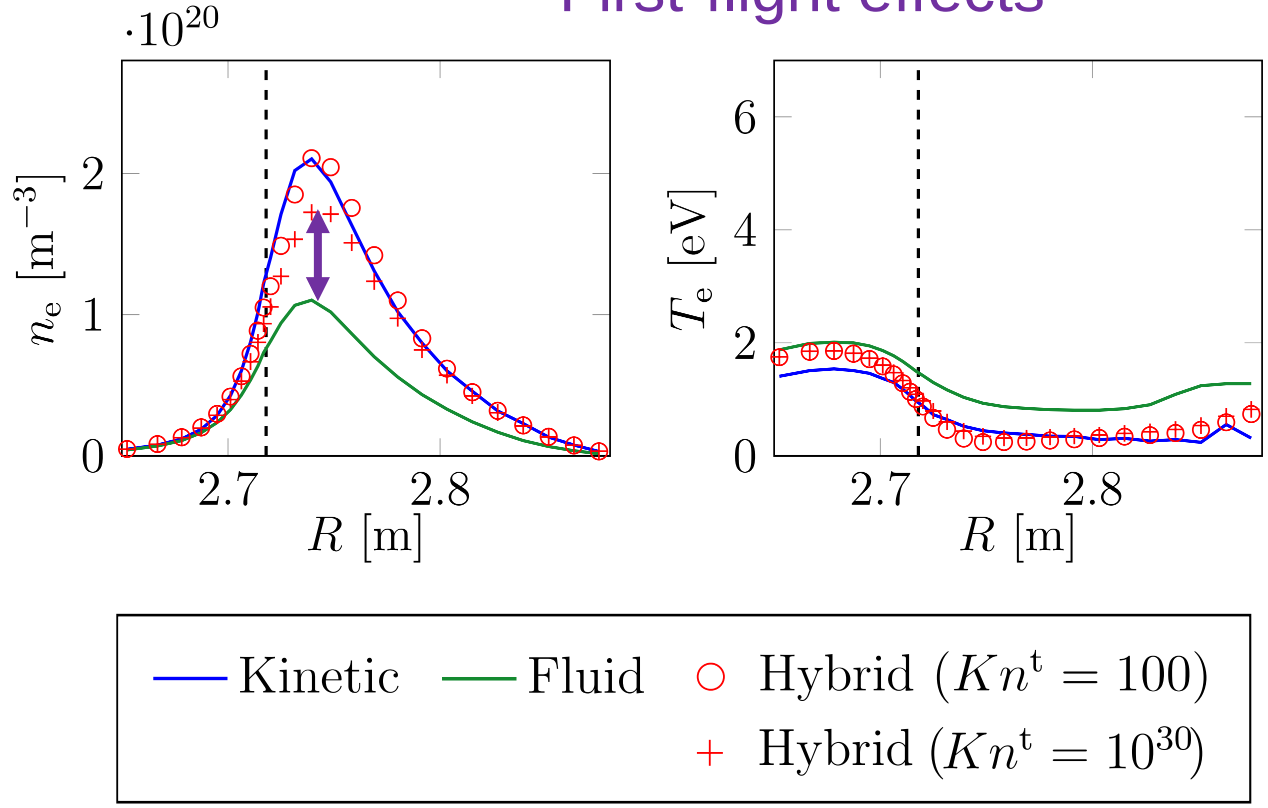

Speed-up compared to simulation with fully kinetic neutrals:

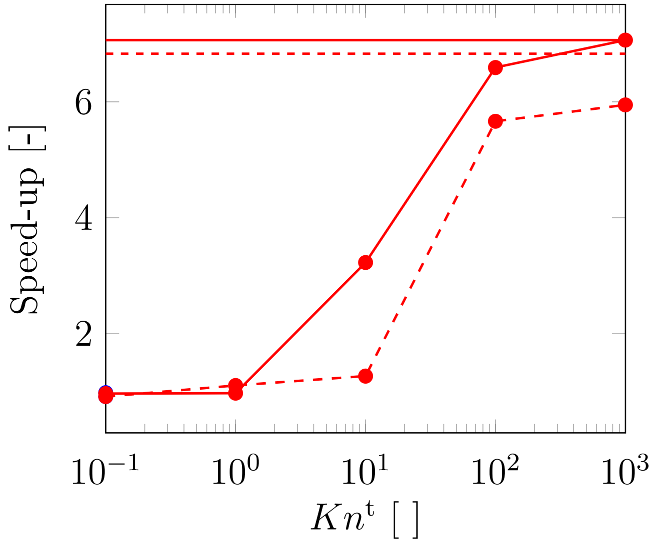

No statistical error correction

With statistical error correction (for $n_{e,ot}$)

KU LEUVEN

Achievements spatially hybrid modeling (SpH)

- Combine AFN model in high-collisional regions with kinetic treatment in low collisional regions [W. Van Uytven, CPP, 2022]
    - Improved accuracy compared to pure fluid
    - Improved speed compared to kinetic (factor 5-20 depending on regime)
- Accurate treatment of molecular and (kinetic) impurity effects
- Fully integrated in extended grids version of SOLPS-ITER for simulations up-to-the-wall

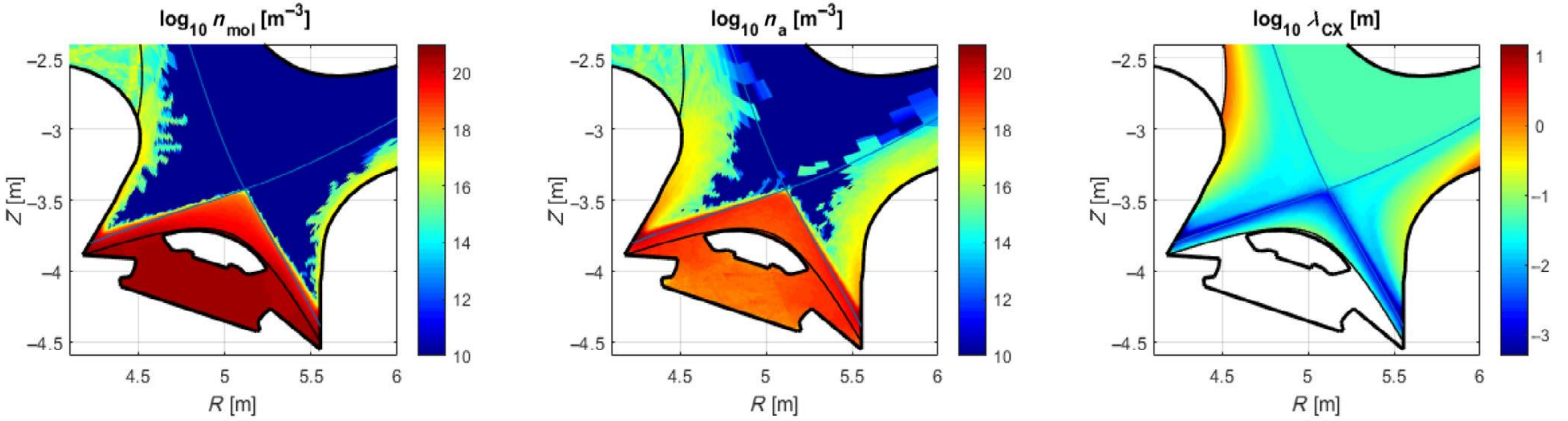

KU LEUVEN

Next steps

- Development of AFN model for molecules
- Development of AFN model for impurity atoms
- More rigorous inclusion of n-n collision effects

KU LEUVEN

References

- N. Horsten et al., Development and assessment of 2D fluid neutral models that include atomic databases and a microscopic reflection model, 2017 Nucl. Fusion 57 116043
- W. Dekeyser et al., Implementation of a 9-point stencil in SOLPS-ITER and implications for Alcator C-Mod divertor plasma simulations, Nuclear Materials and Energy 18 (2019) 125–130
- W. Van Uytven et al., Implementation of a separate fluid-neutral energy equation in SOLPS-ITER and its impact on the validity range of advanced fluid-neutral models, CPP 2020, https://doi.org/10.1002/ctpp.201900147
- W. Dekeyser et al., Plasma edge simulations including realistic wall geometry with SOLPS-ITER, Nuclear Materials and Energy 27 (2021) 100999
- W. Van Uytven et al., Assessment of advanced fluid neutral models for the neutral atoms in the plasma edge and application in ITER geometry, Nucl. Fusion 62 086023
- W. Van Uytven et al., Advanced spatially hybrid fluid-kinetic modelling of plasma-edge neutrals and application to ITER case using SOLPS-ITER, Contrib. Plasma Phys. 2022;e202100191
- W. Van Uytven et al., Discretization error estimation for EU-DEMO plasma-edge simulations using SOLPS-ITER with fluid neutrals, CPP 2024, https://doi.org/10.1002/ctpp.202300125
- N. Vervloesem et al., Error-based grid adaptation methods for plasma edge simulations with SOLPS-ITER,CPP 2024, https://doi.org/10.1002/ctpp.202300126

KU LEUVEN

References

- W. Dekeyser et al., Divertor target shape optimization in realistic edge plasma geometry, Nucl. Fusion 54 (2014) 073022
- M. Blommaert et al., An automated approach to magnetic divertor configuration design, Nucl. Fusion 55 (2015) 013001
- M. Baelmans et al., Achievements and challenges in automated parameter, shape and topology optimization for divertor design, Nucl. Fusion 57 (2017) 036022
- S. Carli et al., Algorithmic Differentiation for adjoint sensitivity calculation in plasma edge codes, Journal of Computational Physics, Volume 491, 15 October 2023, 112403, https://doi.org/10.1016/j.jcp.2023.112403
- S. Carli et al., Bayesian maximum a posteriori-estimation of κ turbulence model parameters using algorithmic differentiation in SOLPS-ITER, https://doi.org/10.1002/ctpp.202100184
- S. Van den Kerkhof et al., Application of an automated grid deformation tool for divertor shape optimization in SOLPS-ITER, CPP 2024, https://doi.org/10.1002/ctpp.202300134
- Maes, V., Bossuyt, I., Vandecasteele, H., Dekeyser, W., Koellermeier, J., Baelmans, M., Samaey, G. (2024). Predicting the statistical error of analog particle tracing Monte Carlo. arXiv. doi: 10.48550/arXiv.2404.00315